Lighting Engineering & Power Engineering
2021, Vol. 60, No. 3, 112–123
https://doi.org/10.33042/2079-424X.2021.60.3.04

OPEN ACCESS

Design and Simulation of a Servo-Drive Motor Using ANSYS Electromagnetics

Vladyslav Pliuhin, Oleksandr Aksonov, Yevgen Tsegelnyk, Sergiy Plankovskyy, Volodymyr Kombarov, and Lidiia Piddubna

O. M. Beketov National University of Urban Economy in Kharkiv, Kharkiv, Ukraine

Article History
Received:
07 November 2021
Accepted:
27 December 2021
Published online:
30 December 2021

Keywords
Servo-drive Motor;
Incorporated Magnets;
ANSYS Simplorer;
Twin Builder;
Motor Parameters

Abstract
The paper is devoted to determining the output parameters of a servomotor, which belongs to synchronous machines with permanent magnets, in order to further determine the characteristics of transient modes in the software package ANSYS Electromagnetics. RMxprt, part of ANSYS Electromagnetics, allows to determine the parameters of windings, losses, motor performance, but requires filling out a form with a complete set of geometric dimensions and winding data. Of course, such data are not available in the motor data sheet, so the first task solved in the paper is to determine all the necessary and sufficient parameters to perform the calculation in RMxprt. The results of the calculations were compared with the measurements on the experimental servomotor EMG-10APA22. This paper shows how to export a servomotor object from RMxprt to the Simplorer workspace, which is also part of the ANSYS Electromagnetics. According to the simulation results in ANSYS Simplorer, the characteristics of the transient modes of the servomotor powered by a stable three-phase source are obtained. Prospects for further research related to the improvement of the simulation model in ANSYS Simplorer are presented.

INTRODUCTION

A servomotor is a motor that allows to control the precise position of the motor shaft as well as the speed and/or acceleration. For this, appropriate sensors and automatic control methods are used. Servomotors used to be auxiliary drives that were designed for machine tool applications [1–3].

Servomotors can be divided into synchronous and asynchronous [4]. But it is always a drive operating under conditions of electronic control of position, speed or torque – or a combination of these parameters. This places very high demands on dynamics, control ranges and/or movement accuracy. Servomotors are usually used in combination with automation and control systems, for example in packaging machines [5].

Synchronous servomotors are drives in which the rotor is synchronously driven by a rotating field in the stator using permanent magnets attached to it. The synchronous motor rotates synchronously with the applied frequency of the rotating field. This version of the drive is powered by a frequency converter that provides a suitable, controlled three-phase current. The servomotors can be adapted to high dynamics or high loads, depending on the application. Typical applications are food processing, construction, automotive, packaging and woodworking [4]. In this regard, the analysis of the parameters and characteristics of the servo motor for subsequent optimization in specific areas of use seems relevant [6–8].

The aim of this paper is to analyze the characteristics of the servo motor used by the authors in the mechanism for moving the axes of a gantry CNC machine in the drive of longitudinal displacements. The obtained data will allow to optimize the machine control system, having previously tested it on a simulation model. In turn, this will avoid costs both when performing tests and selecting associated mechanical components, as well as when setting up a control system.

The portal-type machine, on the basis of which the experimental complex is created, in the factory configuration of the supplier is equipped with a rail-gear transmission on the axes of longitudinal movement X, Y (Fig. 1).

Corresponding author: oleksandr.aksonov@kname.edu.ua (Oleksandr Aksonov)

Cite as: Pliuhin, V., Aksonov, O., Tsegelnyk, Y., Plankovskyy, S., Kombarov, V., & Piddubna, L. (2021). Design and simulation of a servo-drive motor using ANSYS Electromagnetics. *Lighting Engineering & Power Engineering, 60*(3), 112–123. https://doi.org/10.33042/2079-424X.2021.60.3.04

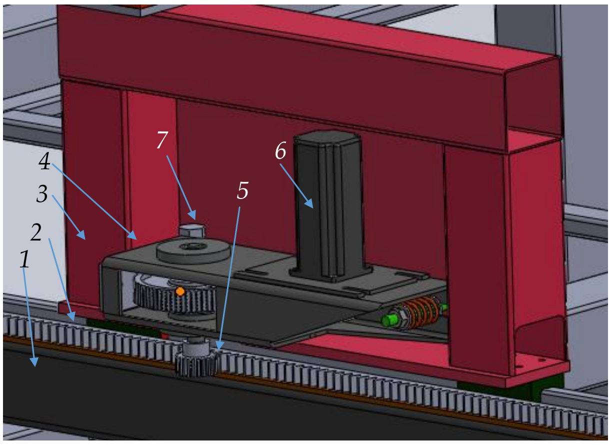

Figure 1. The main elements of the longitudinal drive to move the axis of the portal-type machine

The rack-and-gear *2* is fixed on the frame *1*, and the drive gear *5* is driven by a servo motor *6* through a gear-belt gearbox *4*. The gearbox is mounted on the movable support of the portal-type *3* by means of a rotary axis *7* and the gap in the installed gearbox provides reduction of turns with a gear ratio $R = 72/22 = 3.27$.

Servomotor EMG-10APA22, which is the aim of calculations, is shown in Fig. 2 [9].

The AC EMG-10 servomotor [9] comes standard with a 2500 pulses per revolution. Incremental encoder, runs at a maximum speed of 3000 RPM, provides peak values up to 300% of the rated torque and current values, and has a rated torque of 4.78 Nm with a 1.0 kW power rating. These enclosed and self-cooled motors also provide longer motor life and higher reliability. The EMG-10 AC servomotors enable industrial motion control applications with medium inertia to attain a great combination of speed and positioning functionality.

The passport (rated) data of the servomotor are given in Table 1. Outline drawings of the machine are shown on Fig. 2 (legend corresponds to the dimensions in millimeters given in Table 2).

Fig. 4 shows the rated characteristics of the servomotor operating mode.

Table 1. Rated data of the servomotor EMG-10APA22

Name	Symbol	Value
Rated power, kW	P_n	1000
Line voltage, V	U_n	220
Phase current, A	I_f	6
Rated speed, rpm	n	2000
Frequency, Hz	f	133
Rated torque, Nm	M_n	4,78
Number of phases	m	3
Winding connection	–	star
Winding resistance, Ohm	Z	0,8
Electric Time Constant, ms	T_s	11.57
Inertia, N/s²	J	0.004014

The main parameters, geometric dimensions and winding data of the experimental servomotor are given in Table 3.

PRELIMINARY CALCULATION OF MAIN DIMENSIONS

The data obtained as a result of disassembling the servomotor, as well as the information available on the dimensional drawings, is not enough for the verification calculation in ANSYS, where a complete set of geometric and winding data is required [10–18]. Therefore, preliminary design of the machine must be completed, including the determination of power factor and efficiency targets.

According to the principle of operation, the servomotor belongs to permanent magnet synchronous motors, therefore, the design methodology of such machines will be applied to its calculation [11, 14–16, 19]. The calculation is not performed completely, but only until the point, when the parameters necessary for starting the design in ANSYS are obtained [19]. Thus, it is possible to end with the determination of the basic geometric dimensions and winding data and not perform the calculation of the magnetic circuit, active and inductive resistances of the windings, operating and starting characteristics [20–27]:

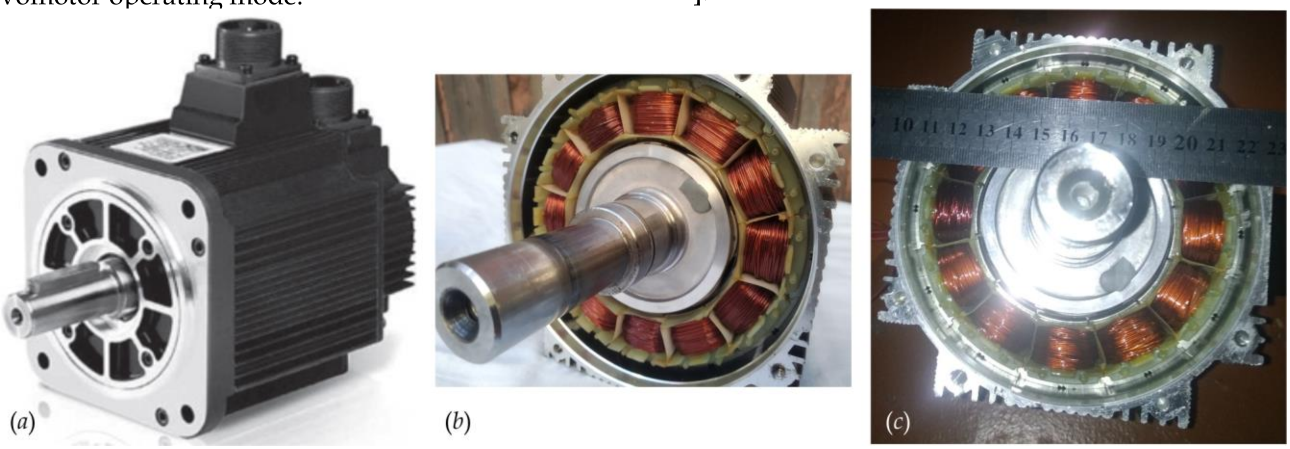

Figure 2. Views of the investigated servomotor: (*a*) – appearance of the EMG-10APA22 servomotor; (*b*) – servomotor with the endshield removed (experimental photo); (*c*) – view of the servomotor coils (photo of the experimental sample)

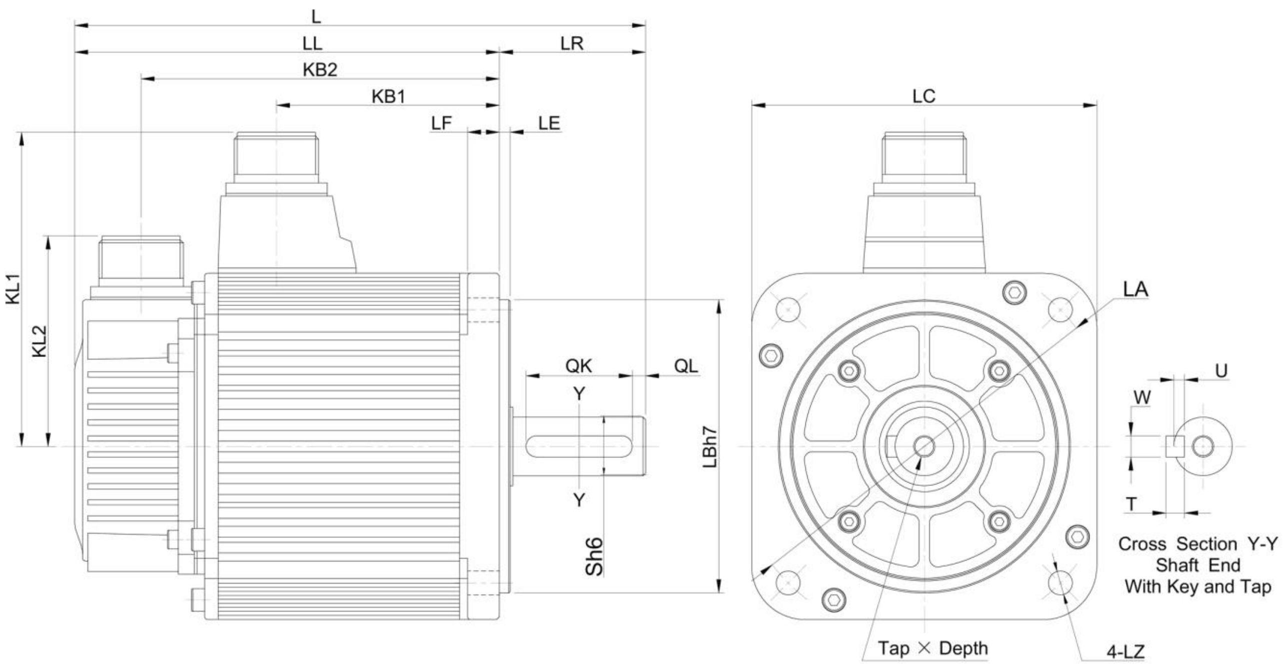

Figure 3. Servomotor EMG-10APA22 outline drawings

Table 2. Servomotor EMG-10APA22 dimensions

L	LL	KB1	KB2	KL1	KL2	Flange Slide							S	Key				
						LR	LE	LF	LC	LA	LB	LZ		QK	QL	W	T	U
215	160	84	135	118	79	55	4	12	130	145	110	9	22	40	5	8	7	4

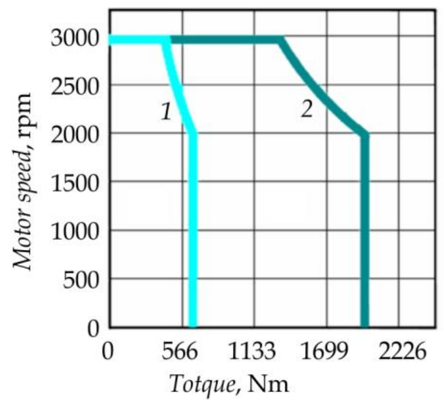

Figure 4. Load characteristics of EMG-10APA22: *1* – continuous working area; *2* – repeatedly working area

Table 3. Servomotor EMG-10APA22 measured dimensions

Name	Symbol	Value
Stator and Rotor core length, mm	L_δ	50
Stator external diameter, mm	D_a	122
Stator inner diameter, mm	D	74
Rotor external diameter, mm	D_r	72
Rotor inner diameter (for the shaft), mm	D_s	36
Number of stator coils	W_c	12
Number of permanent magnets	N_r	8
Magnet thickness, mm	h_m	7
Inductor pole shoe height, mm	h_{p1}	3

- phase voltage

$$U_f = \frac{U_n}{\sqrt{3}};$$

- number of pole pairs

$$p = \frac{60 \cdot f}{n};$$

- rated electromagnetic torque

$$M_n = 9.55 \frac{P_n}{n};$$

- rated phase current

$$I_f = \frac{P_n}{3 \cdot U_f \cdot PF \cdot \eta},$$

where PF is the power factor; η is the efficiency;

- pole pitch

$$\tau = \frac{\pi \cdot D}{2 \cdot p};$$

- pole length (rotor package)

$$L_\delta = \lambda \cdot \tau,$$

where λ is the relative ratio of length and pole pitch;

- air gap magnetic flux

$$\Phi_\delta = \frac{B_\delta \cdot D \cdot L_\delta}{p};$$

- phase EMF (preliminary)

$$E_f = k_e \cdot U_f \text{ ,}$$

where k_e is the magnetic field form factor;

- number of turns per phase

$$W_1 = \frac{E_f}{4.44 \cdot f \cdot \Phi_\delta};$$

- number of turns in a coil

$$W_c = \frac{W_1 \cdot a}{p \cdot q},$$

where a is the number of parallel branches; q is the number of slots per pole and phase.

- cross-section of the winding wire

$$q_{ef} = \frac{I_f}{J_{Cu}},$$

where J_{Cu} is the winding current density;

- elementary conductor cross-section

$$q_{el} = \frac{q_{ef}}{n_{el}},$$

where n_{el} is the number of parallel conductors;

- pole height:

$$h_p = \frac{(D_a - D)}{2} - h_{p1};$$

- number of conductors by pole height:

$$N_c = \frac{h_p - h_{ins}}{d_{el} + \Delta_{ins}},$$

where h_{ins} is the insulation thickness at pole height; Δ_{ins} is the double-sided insulation thickness of winding wire;

In this case, the total thickness of the pole window will be:

$$N_{cw} = \left(\frac{W_c}{N_c} + 1\right) \cdot (d_{el} + \Delta_{ins});$$

- pole thickness

$$b_p = \frac{0.5 \cdot \pi \cdot (D_a + D)}{N_c} - N_{cw} - \Delta_c,$$

where Δ_c is the air gap between coils.

The calculation results of the servomotor, performed according to the presented formulas, are summarized in Table 4.

The received data is now enough to continue the calculation of the parameters and characteristics of the servomotor in RMxprt. In the presented paper, only key formulas are given.

Table 4. Servomotor parameters in addition to the rated data

Name	Value
Phase voltage, V	127
Number of poles	8
Poles pitch, mm	29
Air gap flux density, T	0.75
Air gap magnetic flux, Wb	0.000694
Number of slots per pole and phase	1
Number of parallel branches	1
Phase EMF, V	123
Number of turns in a coil	75
Number of elementary conductors	2
Conductor section, mm^2	0.636
Conductor diameter, mm	0.9
Double-sided conductor insulation thickness, mm	0.065
Pole height, mm	21
Pole thickness, mm	13
Insulation thickness along the pole height, mm	5
Total thickness of the pole window, mm	6
Air gap between coils, mm	7
Power factor	0.61
Efficiency	0.72
Field shape factor	0.97
Ratio between stator diameter and pole pitch	1.7

A detailed calculation was performed by the authors in a Python program [28, 29]. This approach of preliminary determination of parameters was given the author's name "*Python Hot Start*".

PARAMETERS CALCULATION IN ANSYS RMXPRT

ANSYS RMxprt it is needed to select the IPM Synchronous Motor (Incorporated Permanent Magnets) project type that matches the servomotor being tested (Fig. 5).

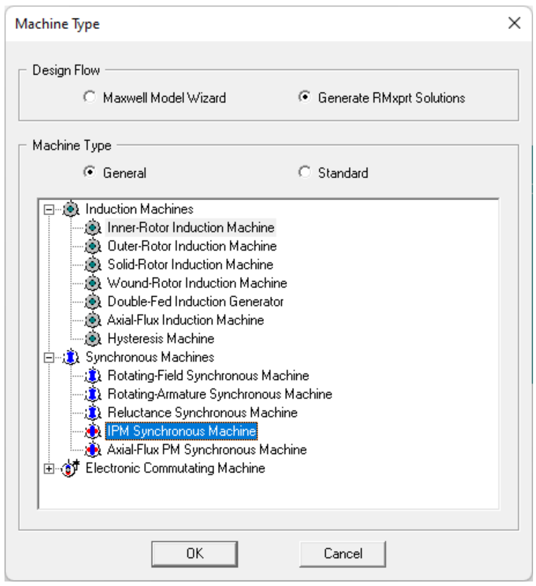

Figure 5. ANSYS RMxprt: project type selection

Next, in the tree of the project manager, it is need sequentially fill in the tables of motor parameters and select the required materials (Fig. 6). Let's consider each of the steps of entering parameters [19].

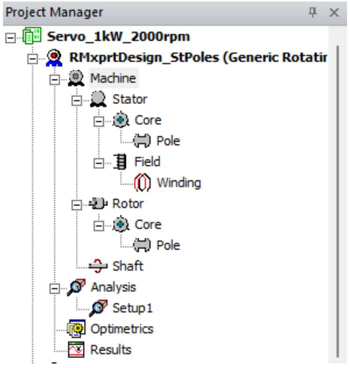

Figure 6. ANSYS RMxprt: machine characteristics tree

Machine. This section (Fig. 7) selects the stator type and rotor configuration. For the problem under consideration, a salient-pole stator with an internal rotor with built-in permanent magnets was chosen.

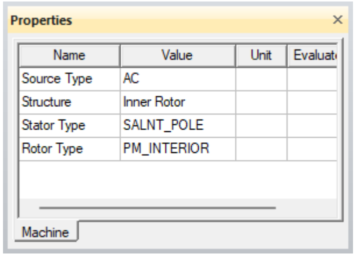

Properties

Name	Value	Unit	Evaluat
Source Type	AC		
Structure	Inner Rotor		
Stator Type	SALNT_POLE		
Rotor Type	PM_INTERIOR		

Machine

Figure 7. ANSYS RMxprt: global machine properties

Stator. Only the number of poles is specified on the stator properties tab (Fig. 8).

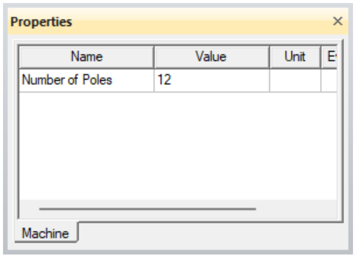

Properties

Name	Value	Unit	E
Number of Poles	12		

Machine

Figure 8. ANSYS RMxprt: stator properties

Stator Core. For the stator, the previously calculated geometric dimensions (Fig. 9), the steel filling factor are indicated, the steel material is selected from the program database (it is possible to create user material by setting the magnetization curve) and the pole type is selected (Fig. 10).

Stator Core Pole. In this section, the dimensions of the pole are set. The pole suggested by the program (Fig. 10) does not correspond to the real pole of the tested servomotor, however, by specifying the dimensions of the pole, shoe and the length of the arcs, an acceptable match can be achieved (Fig. 11, 12).

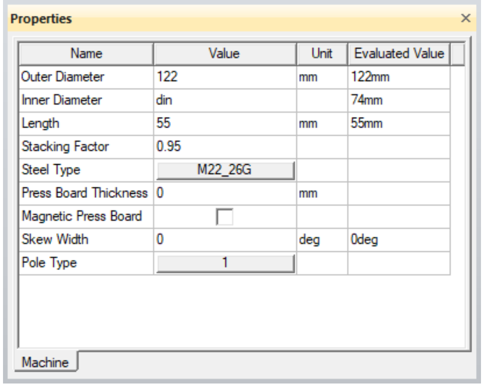

Properties

Name	Value	Unit	Evaluated Value
Outer Diameter	122	mm	122mm
Inner Diameter	din		74mm
Length	55	mm	55mm
Stacking Factor	0.95		
Steel Type	M22_26G		
Press Board Thickness	0	mm	
Magnetic Press Board	☐		
Skew Width	0	deg	0deg
Pole Type	1		

Machine

Figure 9. ANSYS RMxprt: stator core parameters

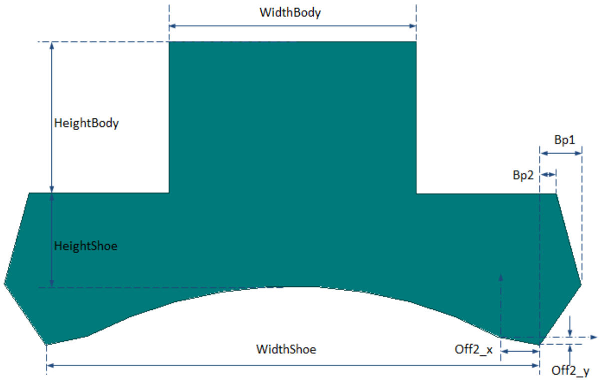

Figure 10. ANSYS RMxprt: sketch of poles

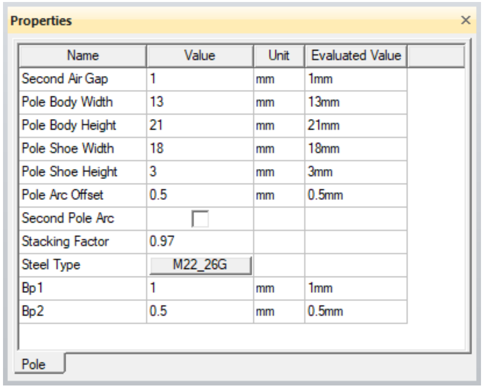

Properties

Name	Value	Unit	Evaluated Value
Second Air Gap	1	mm	1mm
Pole Body Width	13	mm	13mm
Pole Body Height	21	mm	21mm
Pole Shoe Width	18	mm	18mm
Pole Shoe Height	3	mm	3mm
Pole Arc Offset	0.5	mm	0.5mm
Second Pole Arc	☐		
Stacking Factor	0.97		
Steel Type	M22_26G		
Bp1	1	mm	1mm
Bp2	0.5	mm	0.5mm

Pole

Figure 11. ANSYS RMxprt: inductor pole parameters

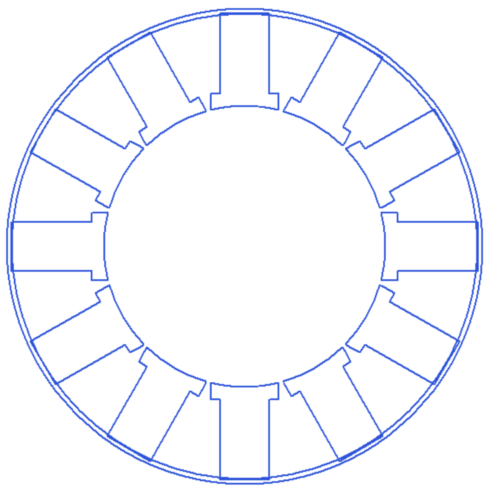

Figure 12. ANSYS RMxprt: sketch of a stator with poles

Stator Field. The coil parameters window (Fig. 13) shows the pole insulation, power supply efficiency and field current.

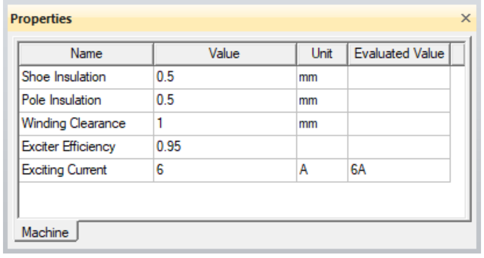

Properties

Name	Value	Unit	Evaluated Value
Shoe Insulation	0.5	mm	
Pole Insulation	0.5	mm	
Winding Clearance	1	mm	
Exciter Efficiency	0.95		
Exciting Current	6	A	6A

Machine

Figure 13. ANSYS RMxprt: excitation system characteristics

Stator Field Winding. For the coil winding, its type is selected (the program includes coils with rectangular conductors wound flat and on an edge), the number of conductors, their dimensions, as well as the material of the winding wire (Fig. 14).

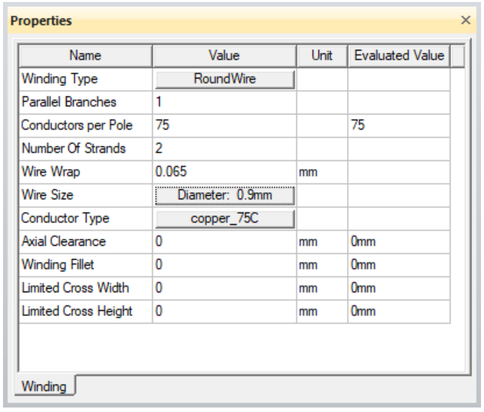

Properties

Name	Value	Unit	Evaluated Value
Winding Type	RoundWire		
Parallel Branches	1		
Conductors per Pole	75		75
Number Of Strands	2		
Wire Wrap	0.065	mm	
Wire Size	Diameter: 0.9mm		
Conductor Type	copper_75C		
Axial Clearance	0	mm	0mm
Winding Fillet	0	mm	0mm
Limited Cross Width	0	mm	0mm
Limited Cross Height	0	mm	0mm

Winding

Figure 14. ANSYS RMxprt: winding parameters of inductors

Rotor. For the rotor, as before for the stator, the number of poles is indicated (Fig. 15).

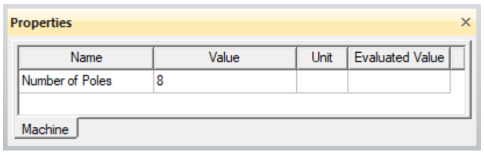

Properties

Name	Value	Unit	Evaluated Value
Number of Poles	8		

Machine

Figure 15. ANSYS RMxprt: rotor properties

Rotor Core. In the parameters of the rotor core, the outer diameter was given in the form of a formula (Fig. 16), relating its value to the air gap and the inner diameter of the stator. The rotor length, core material and pole type are also indicated. Among the types of poles available in the program, the one corresponding to the prototype was chosen (Fig. 17).

Rotor Core Pole. In this tab one can set the dimensions and select the material of the permanent magnets. (Fig. 18).

After the performed operations, a complete sketch of the servo motor becomes available (Fig. 19).

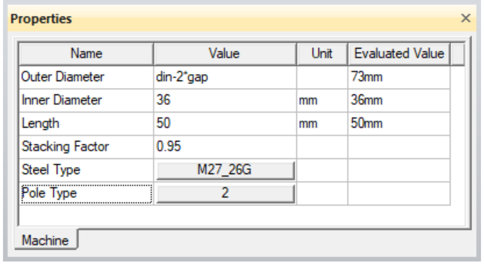

Properties

Name	Value	Unit	Evaluated Value
Outer Diameter	din-2*gap		73mm
Inner Diameter	36	mm	36mm
Length	50	mm	50mm
Stacking Factor	0.95		
Steel Type	M27_26G		
Pole Type	2		

Machine

Figure 16. ANSYS RMxprt: rotor core parameters

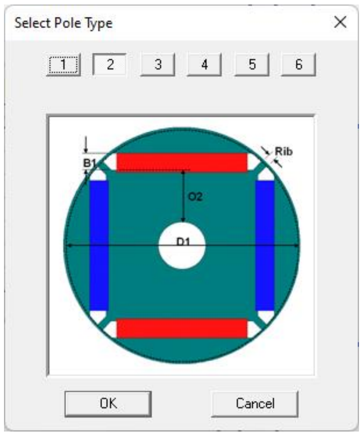

Figure 17. ANSYS RMxprt: selection of the permanent magnets type

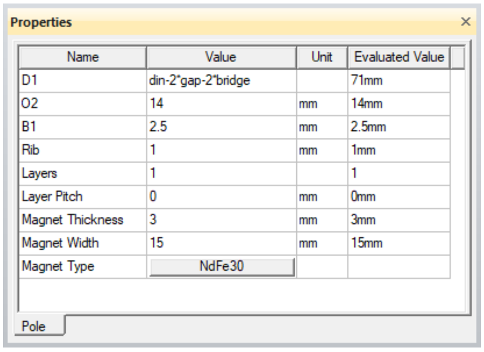

Properties

Name	Value	Unit	Evaluated Value
D1	din-2*gap-2*bridge		71mm
O2	14	mm	14mm
B1	2.5	mm	2.5mm
Rib	1	mm	1mm
Layers	1		1
Layer Pitch	0	mm	0mm
Magnet Thickness	3	mm	3mm
Magnet Width	15	mm	15mm
Magnet Type	NdFe30		

Pole

Figure 18. ANSYS RMxprt: permanent magnets dimensions

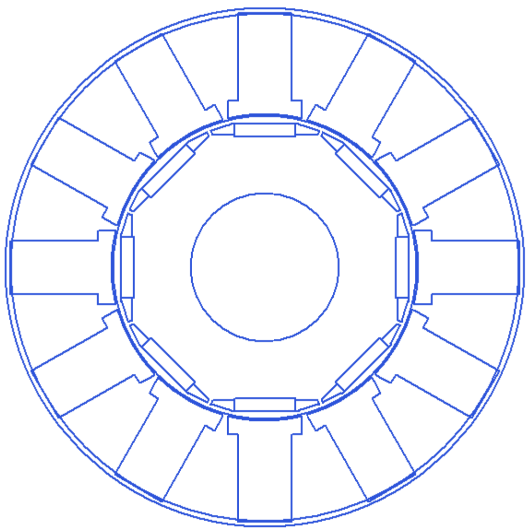

Figure 19. ANSYS RMxprt: servo motor sketch

Shaft. For the shaft, the presence of a magnetic material is selected in the properties, ventilation and friction losses in the bearings are set at the nominal speed (Fig. 20).

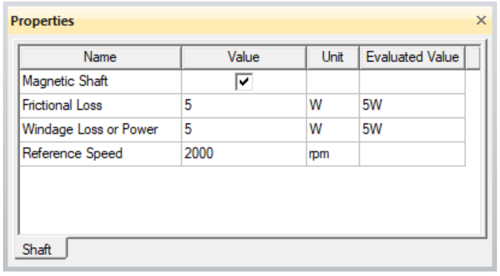

Properties

Name	Value	Unit	Evaluated Value
Magnetic Shaft	☑		
Frictional Loss	5	W	5W
Windage Loss or Power	5	W	5W
Reference Speed	2000	rpm	

Shaft

Figure 20. ANSYS RMxprt: shaft parameters

Analysis. The analysis tab initially does not contain attached properties, in order to create them, after clicking the right mouse button, the context menu item "Add Solution Setup" is selected.

Analysis Setup. This group of properties is final and consists of two tabs. The first (Fig. 21*a*) selects the operating mode and nominal motor data, and the second (Fig. 21*b*) selects the operating frequency and power factor.

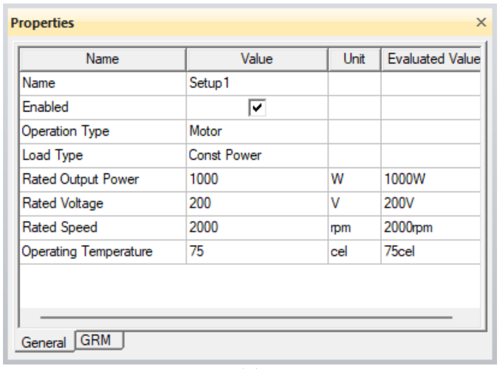

Properties

Name	Value	Unit	Evaluated Value
Name	Setup1		
Enabled	☑		
Operation Type	Motor		
Load Type	Const Power		
Rated Output Power	1000	W	1000W
Rated Voltage	200	V	200V
Rated Speed	2000	rpm	2000rpm
Operating Temperature	75	cel	75cel

General GRM

(*a*)

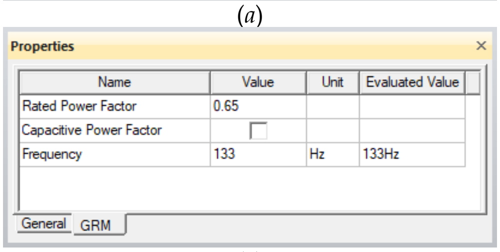

Properties

Name	Value	Unit	Evaluated Value
Rated Power Factor	0.65		
Capacitive Power Factor	☐		
Frequency	133	Hz	133Hz

General GRM

(*b*)

Figure 21. ANSYS RMxprt: solver properties: (*a*) solver properties (part 1); (*b*) solver properties (part 2)

The results of the analysis are shown below and show satisfactory convergence with the servo motor nameplate data. In particular, the main key parameters coincided (torque and phase current), and the rest are within acceptable limits in terms of the requirements for electric machines in general (magnetic flux density, current density, losses, efficiency).

Fig. 22–26 shows the servomotor characteristics obtained in RMxprt.

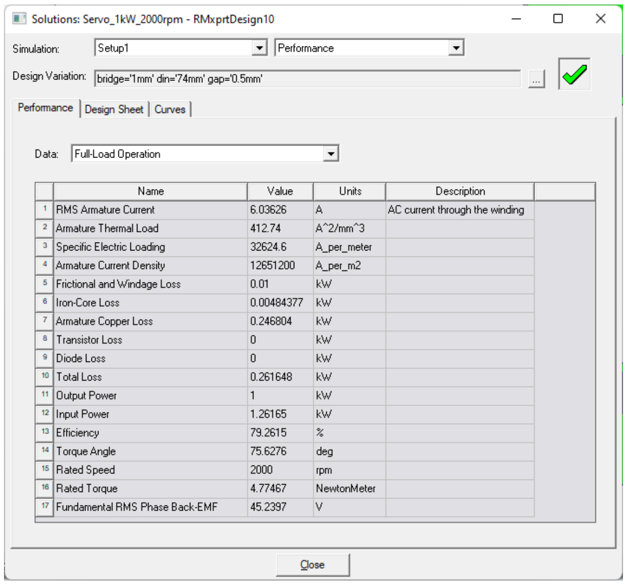

Solutions: Servo_1kW_2000rpm - RMxprtDesign10

Simulation: Setup1 Performance

Design Variation: bridge='1mm' din='74mm' gap='0.5mm'

Performance | Design Sheet | Curves

Data: Full-Load Operation

	Name	Value	Units	Description
1	RMS Armature Current	6.03626	A	AC current through the winding
2	Armature Thermal Load	412.74	A^2/mm^3	
3	Specific Electric Loading	32624.6	A_per_meter	
4	Armature Current Density	12651200	A_per_m2	
5	Frictional and Windage Loss	0.01	kW	
6	Iron-Core Loss	0.00484377	kW	
7	Armature Copper Loss	0.246804	kW	
8	Transistor Loss	0	kW	
9	Diode Loss	0	kW	
10	Total Loss	0.261648	kW	
11	Output Power	1	kW	
12	Input Power	1.26165	kW	
13	Efficiency	79.2615	%	
14	Torque Angle	75.6276	deg	
15	Rated Speed	2000	rpm	
16	Rated Torque	4.77467	NewtonMeter	
17	Fundamental RMS Phase Back-EMF	45.2397	V	

Close

Figure 22. ANSYS RMxprt: Servomotor calculation report (data under load)

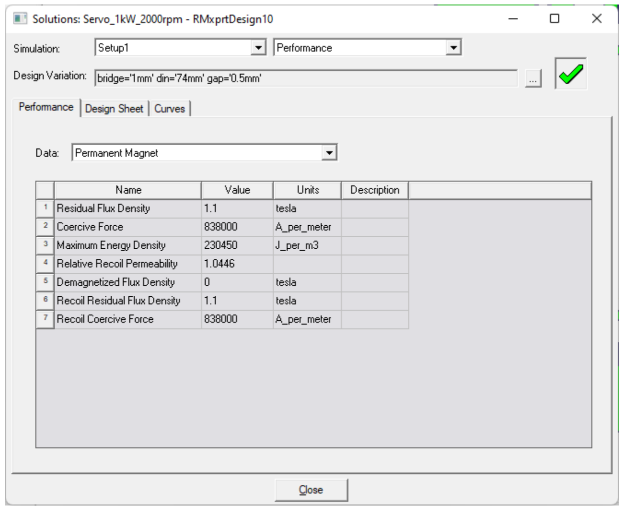

Solutions: Servo_1kW_2000rpm - RMxprtDesign10

Simulation: Setup1 Performance

Design Variation: bridge='1mm' din='74mm' gap='0.5mm'

Performance | Design Sheet | Curves

Data: Permanent Magnet

	Name	Value	Units	Description
1	Residual Flux Density	1.1	tesla	
2	Coercive Force	838000	A_per_meter	
3	Maximum Energy Density	230450	J_per_m3	
4	Relative Recoil Permeability	1.0446		
5	Demagnetized Flux Density	0	tesla	
6	Recoil Residual Flux Density	1.1	tesla	
7	Recoil Coercive Force	838000	A_per_meter	

Close

Figure 23. ANSYS RMxprt: permanent magnet solver report

TRANSIENT MODELING IN ANSYS SIMPLORER

The ANSYS Simplorer software package allows to simulate the transient characteristics of electrical machines not only on the basis of mathematical models set by differential equations or built-in machine models, but also in coupling with previous projects in RMxprt or ANSYS Maxwell 2D/3D [19]. That approach in ANSYS called Twin Builder. To solve this problem, a Twin Builder component was inserted into the Simplorer worksheet for coupling simulation analysis of the servomotor dynamic modes based on a machine object from the RMxprt project.

In this paper, the first phase of the problem is solved – to link the RMxprt project with the Simplorer power supply and obtain the output characteristics.

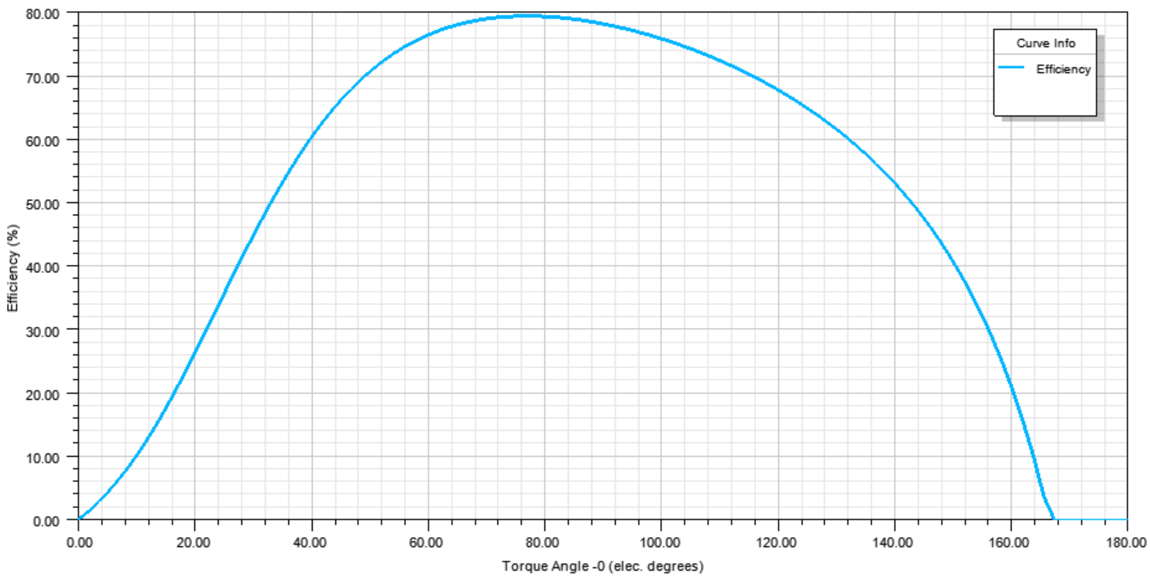

Figure 24. Efficiency vs Torque Angle

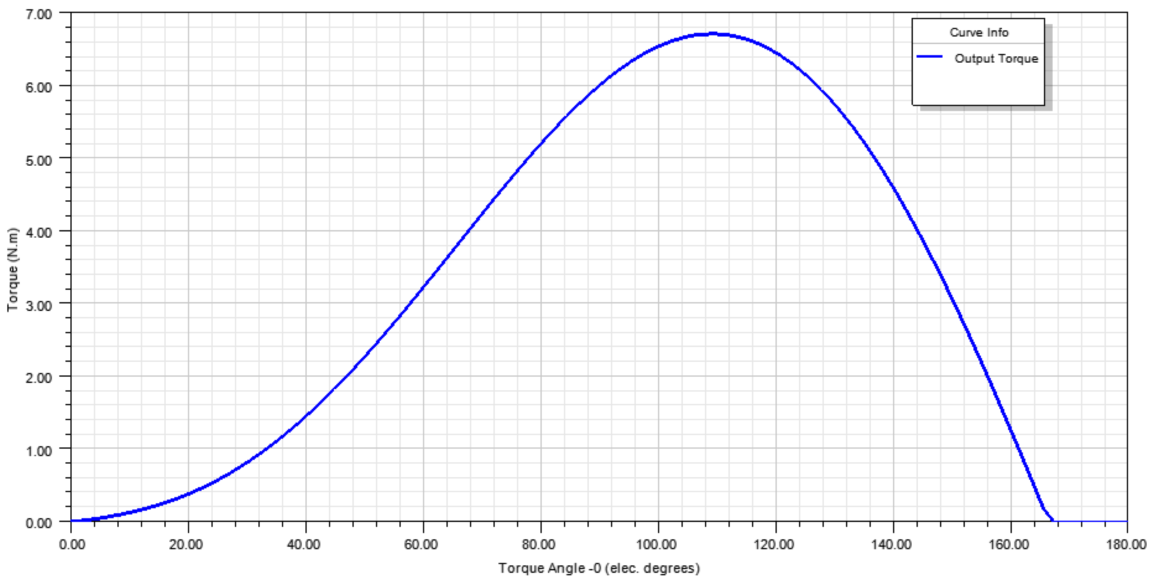

Figure 25. Output Torque vs Torque Angle

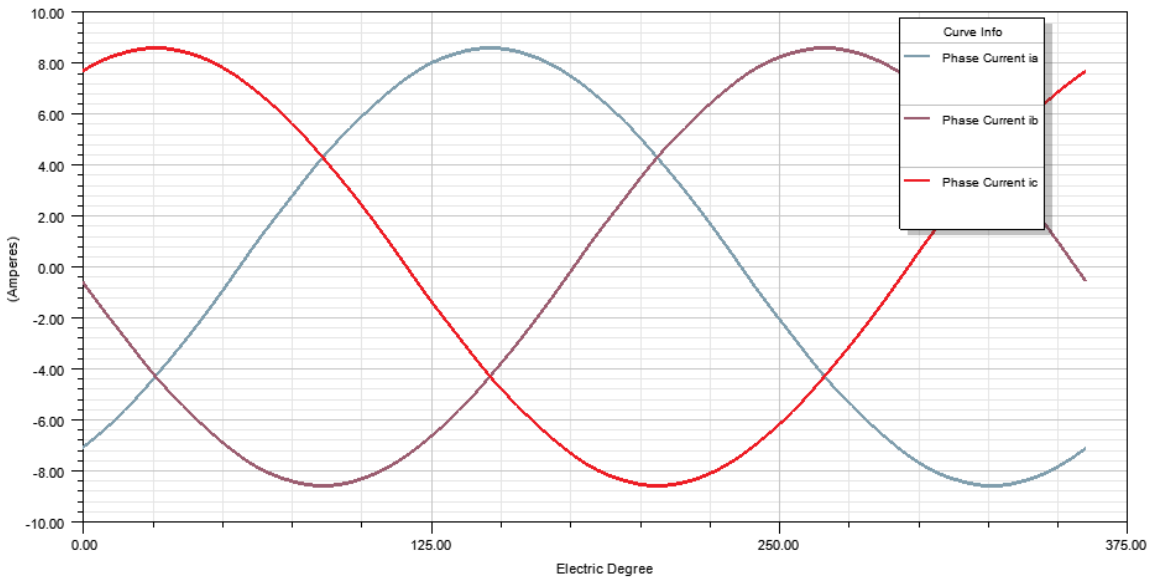

Figure 26. Winding Currents under Load

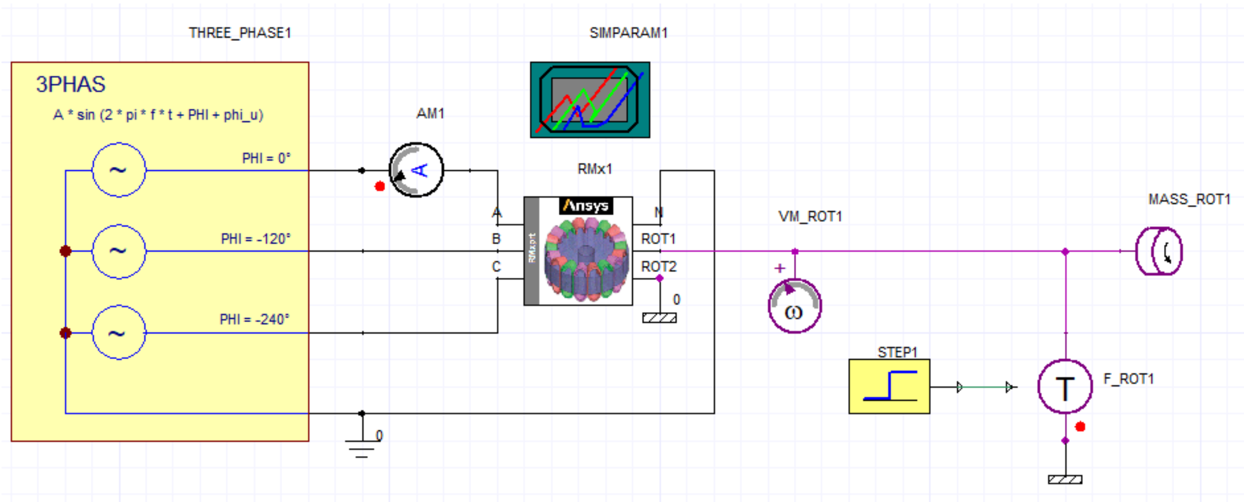

Figure 27. ANSYS Simplorer: simulated servomotor with a stable power supply

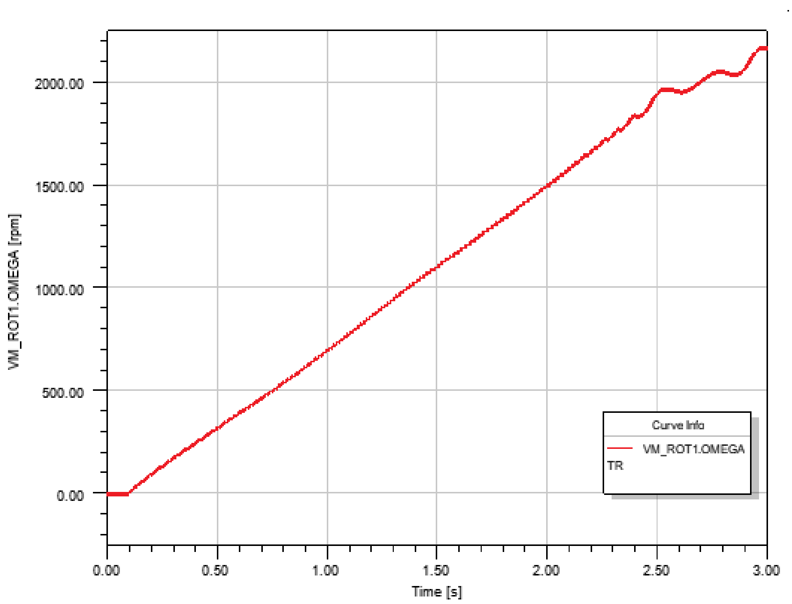

Figure 28. Rotational Speed vs Time

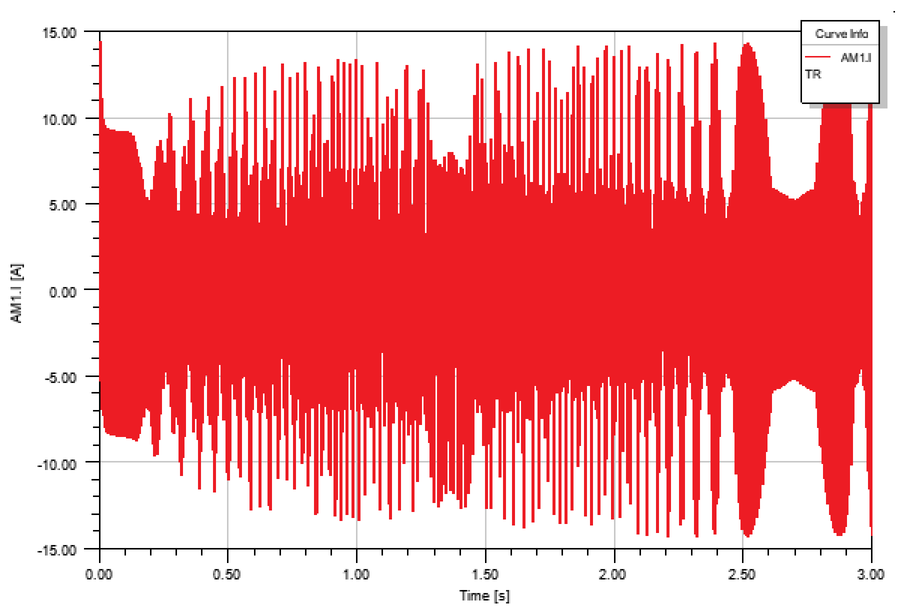

Figure 29. Phase Current vs Time

In future works, more complex circuits for simulating transient processes in a servo motor, taking into account power from a frequency converter, using a speed sensor and variable loads, will be shown.

Fig. 27 shows a simulation model, which shows a three-phase power supply *3PHAS*, a servo motor object from RMxprt *RMx1*, an amperemeter *AM1*, a tachometer *VM_ROT1*, a rotor inertia source *MASS_ROT1*, a step load generator *STEP1*, and a torque sensor *F_ROT1*.

In the settings of the three-phase power supply and the element characterizing the inertia value, the data from the project were passed. The rated load in the STEP1 block was applied at the time 0.1 s. The simulated characteristics are shown in Fig. 28 and Fig. 29.

The values of the rotor speed and the value of the effective value of the stator winding phase current, obtained during the stabilization of the transient process correspond to the values obtained both as a result of preliminary design and the rated data of the servomotor.

CONCLUSIONS

The use of the ANSYS software package for the analysis of parameters and characteristics of electrical machines in general and the servomotor considered in this article in particular is justified in cases where geometric and winding data are known. Therefore, in this article, the problem of preliminary design of a servomotor was solved for subsequent calculations in ANSYS.

The software module RMxprt, included in ANSYS Electromagnetics software, allows, after the transformations shown in this article, to obtain, based on a standard design of a synchronous machine with built-in permanent magnets, a design of a servomotor with salient stator poles and a concentrated winding. The criterion for the correctness of the calculations is the maximum approximation of the key characteristics to the rated data of the tested motor. Thus, the target values of the phase current of 6 A, the rotation speed of 2000 rpm, the torque on the shaft of 4.78 Nm and other parameters were achieved.

The Simplorer software module, included in ANSYS Electromagnetics, made it possible to simulate the dynamic modes of a servomotor without using the standard blocks of electrical machines and mathematical models. Instead, an alternative way of embedding a servomotor object, calculated in RMxprt, into the Simplorer simulation field was shown, and then obtaining the transient characteristics of the machine.

In this paper, we examined the simulation of the dynamic modes of a servo motor in ANSYS Simplorer using a stable three-phase power supply (amplitude 127 V, frequency 133 Hz), considering the rated load connection during the acceleration phase. In future work, it is planned to perform a detailed simulation of a servomotor using an embedded servomotor object from RMxprt and using power from a frequency converter together with implementing speed feedback.

DISCLOSURE STATEMENT

No potential conflict of interest was reported by the author(s).

REFERENCES

1. Nicolescu, A., Avram, C., & Ivan, M. (2014). Optimal servomotor selection algorithm for industrial robots and machine tools NC axis. *Proceedings in Manufacturing Systems, 9*(2), 105–114. http://icmas.eu/Journal_archive_files/Vol_9-Issue2_2014_PDF/105-114_Nicolescu.pdf

2. Yamazaki, T. (2017). Experimental study on dynamic behavior of high precision servo motor for machine tools. *Applied Mechanics and Materials, 863*, 224–228. https://doi.org/10.4028/www.scientific.net/AMM.863.224

3. Kombarov, V., Sorokin, V., Tsegelnyk, Y., Plankovskyy, S., Aksonov, Y., & Fojtů, O. (2021). Numerical control of machining parts from aluminum alloys with sticking minimization. *International Journal of Mechatronics and Applied Mechanics, 1*(9), 209–216. https://doi.org/10.17683/ijomam/issue9.30

4. Abdul Ali, A.W., Abdul Razak, F.A., & Hayima, N. (2020). A review on the AC servo motor control systems. *ELEKTRIKA – Journal of Electrical Engineering, 19*(2), 22–39. https://doi.org/10.11113/elektrika.v19n2.214

5. Hossain, A., & Rasheduzzaman, M. (2011). Integrating servomotor concepts into mechatronics engineering technology curriculum emphasizing high speed packaging machinery. In *2011 ASEE Annual Conference & Exposition* (p. 22.915). ASEE. https://doi.org/10.18260/1-2--18244

6. Voss, W. (2007). *A Comprehensible Guide to Servo Motor Sizing*. Copperhill Media.

7. Vagati, A., Fratta, A., Franceschini, G., & Rosso, P. (1996). AC motors for high-performance drives: a design-based comparison. *IEEE Transactions on Industry Applications, 32*(5), 1211–1219. https://doi.org/10.1109/28.536885

8. Huang, C., Lei, F., Han, X., & Zhang, Z. (2019). Determination of modeling parameters for a brushless DC motor that satisfies the power performance of an electric vehicle. *Measurement and Control, 52*(7-8), 765–774. https://doi.org/10.1177/0020294019842607

9. ESTUN. (2021). AC Servo Motor. http://estun.com.ua/pdf/ac_servo_motor.pdf

10. Shinde, P.S., Thosar, A.G., & Ratnani, P.L. (2015). Design of permanent magnet synchronous motor. *International Journal of Scientific & Engineering Research, 6*(1), 107–110. https://ijser.org/researchpaper/design-of-permanent-magnet-synchronous-motor.pdf

11. Shen, Q., Sun, N., Zhao, G., Han, X., & Tang, R. (2010). Design of a permanent magnet synchronous motor and performance analysis for subway. In *2010 Asia-Pacific Power and Energy Engineering Conference* (pp. 1–4). IEEE. https://doi.org/10.1109/APPEEC.2010.5449212

12. Isfahani, A.H., & Sadeghi, S. (2008). Design of a permanent magnet synchronous machine for the hybrid electric vehicle. *World Academy of Science, Engineering and Technology, 45*, 566–570. https://doi.org/10.5281/zenodo.1332212

13. Panigrahi, B.P., Patra, K.C., Subbarao, V., & Prasad, D. (1999). Design of a permanent magnet synchronous motor. *Electric Machines & Power Systems, 27*(7), 771–779. https://doi.org/10.1080/073135699269000

14. Akar, M., & Temiz, I. (2007). Motion controller design for the speed control of DC servo motor. *International Journal of Applied Mathematics and Informatics, 4*(1), 131–137. http://www.wseas.us/journals/ami/ami-19.pdf

15. Zhang, Y., Yang, Z., Yu, M., Lu, K., Ye, Y., & Liu, X. (2011). Analysis and design of double-sided air core linear servo motor with trapezoidal permanent magnets. *IEEE Transactions on Magnetics, 47*(10), 3236–3239. https://doi.org/10.1109/TMAG.2011.2156398

16. Hanselman, D.C. (2003). *Brushless Permanent Magnet Motor Design*. The Writers' Collective.

17. Chenwei, Y., Fei, D., Yi, A., & Fengqing, Z. (2021). Design and analysis of permanent magnet synchronous servo motor with low rotational inertia and high torque density. *Journal of Physics: Conference Series, 1965*(1), 012010. https://doi.org/10.1088/1742-6596/1965/1/012010

18. Deeb, R., Janda, M., & Makki, Z. (2012). Comparison of 2D and 3D FEM analysis of the magnetic field in a PM servo motor. *Electrical Engineering, 72*, 297–309. https://yadda.icm.edu.pl/baztech/element/bwmeta1.element.baztech-2e33696a-32cc-4941-8c0a-4369c102e081/c/deeb_ramia_comparison_72_2012.pdf

19. Pliugin, V., Petrenko, O., Grinina, V., Grinin, O., & Yehorov, A. (2017). Imitation model of a high-speed induction motor with frequency control. *Electrical Engineering & Electromechanics*, (6), 14–20. https://doi.org/10.20998/2074-272X.2017.6.02

20. Gope, D., & Goel, S.K. (2021). Design optimization of permanent magnet synchronous motor using Taguchi method and experimental validation. *International Journal of Emerging Electric Power Systems, 22*(1), 9–20. https://doi.org/10.1515/ijeeps-2020-0169

21. Luu, P.T., Lee, J.Y., Lee, J.H., & Woo, B.C. (2019). Design and analysis of a permanent magnet synchronous motor considering axial asymmetric position of rotor to stator. *Energies, 12*(24), 4816. https://doi.org/10.3390/en12244816

22. Ding, W.T., An, L.X., Wang, C.M., Huang, Y.P., Long, T., & Jiang, M.L. (2015). Multidisciplinary integrated simulation and design optimization framework for electromechanical servo system. *Applied Mechanics and Materials, 704*, 263–269. https://doi.org/10.4028/www.scientific.net/AMM.704.263

23. Lu, H., & Guru, A.K. (2013). Modeling conducted emissions in servo drives. In *2013 IEEE 8th Conference on Industrial Electronics and Applications (ICIEA)* (pp. 999–1004). IEEE. https://doi.org/10.1109/ICIEA.2013.6566513

24. Lei, H., Chen, Y., Chen, D., Li, Z., & Zhu, H. (2021). Design and analysis of permanent magnet AC servo motor based on ANSYS. *Journal of Physics: Conference Series, 1754*(1), 012151. https://doi.org/10.1088/1742-6596/1754/1/012151

25. Krishnan, R. (1987). Selection criteria for servo motor drives. *IEEE Transactions on Industry Applications, IA-23*(2), 270–275. https://doi.org/10.1109/TIA.1987.4504902

26. Qiu, H., Zhang, Y., Yang, C., & Yi, R. (2020). Analysis of permanent magnet servo motor performance with different semi-ferromagnetic sleeve materials. *Transactions of the Canadian Society for Mechanical Engineering, 45*(1), 11–21. https://doi.org/10.1139/tcsme-2019-0201

27. Shavkun, V. (2020). Methodology for the assessment of the operation reliability of pulling electric machines of city electric transport. *Lighting Engineering & Power Engineering, 58*(2), 58–64. https://doi.org/10.33042/2079-424X-2020-2-58-13-19 (in Ukrainian)

28. Pliuhin, V., Korobka, V., Karyuk, A., Pan, M., & Sukhonos, M. (2019). Using Azure Machine Learning Studio with Python scripts for induction motors optimization web-deploy project. In *2019 IEEE International Scientific-Practical Conference Problems of Infocommunications, Science and Technology (PIC S&T)* (pp. 631–634). IEEE. https://doi.org/10.1109/PICST47496.2019.9061447

29. Pliuhin, V., Sukhonos, M., & Bileckiy, I. (2020). Object oriented mathematical modeling of electrical machines. In *2020 IEEE 4th International Conference on Intelligent Energy and Power Systems (IEPS)* (pp. 267–272). IEEE. https://doi.org/10.1109/IEPS51250.2020.9263158

Проектування та моделювання сервоприводного двигуна за допомогою використання ANSYS Electromagnetics

Владислав Плюгін, Олександр Аксьонов, Євген Цегельник, Сергій Планковський, Володимир Комбаров, Лідія Піддубна

Анотація. Стаття присвячена визначенню вихідних параметрів серводвигуна, який відноситься до синхронних машин з постійними магнітами, з метою подальшого визначення характеристик динамічних режимів в програмному пакеті ANSYS Electromagnetics. Програма RMxprt, яка входить до ANSYS Electromagnetics, дозволяє визначити параметри обмоток, втрати, робочі характеристики двигуна, але вимагає заповнення формуляру з повним набором геометричних розмірів та обмоткових даних. Звичайно, такі дані відсутні у паспорті двигуна, тому перша задача, яка вирішена у статті – це визначення всіх необхідних і достатніх параметрів для виконання розрахунку в RMxprt. Результати розрахунків були порівняні із вимірюваннями за допомогою експериментального зразку серводвигуна моделі EMG-10APA22. У статті показано, як виконати експорт об'єкту серводвигуна з RMxprt у робочий простір програми Simplorer, яка також входить до пакету ANSYS Electromagnetics. За результатами моделювання в ANSYS Simplorer отримано характеристики перехідних режимів серводвигуна при живленні від стабільного трифазного джерела. Показано перспективи подальших досліджень, пов'язаних з удосконаленням імітаційної моделі в ANSYS Simplorer.

Ключові слова: сервоприводний двигун, вбудовані магніти, ANSYS Simplorer, Twin Builder, параметри двигуна.

NOTES ON CONTRIBUTORS

Vladyslav Pliuhin
vladyslav.pliuhin@kname.edu.ua

D.Sc., Professor
Department of Urban Power Supply Systems and Power Consumption
O. M. Beketov National University of Urban Economy in Kharkiv, Kharkiv, Ukraine
iD https://orcid.org/0000-0003-4056-9771
P https://publons.com/researcher/F-4627-2018/
SC https://scopus.com/authid/detail.uri?authorId=57204286328

Oleksandr Aksonov
oleksandr.aksonov@kname.edu.ua

Postgraduate student
Department of Urban Power Supply Systems and Power Consumption
O. M. Beketov National University of Urban Economy in Kharkiv, Kharkiv, Ukraine
iD https://orcid.org/0000-0002-1870-524X

Yevgen Tsegelnyk
y.tsegelnyk@kname.edu.ua

Ph.D., Associate Professor
Department of Automation and Computer-Integrated Technologies
O. M. Beketov National University of Urban Economy in Kharkiv, Kharkiv, Ukraine
iD https://orcid.org/0000-0003-1261-9890
P https://publons.com/researcher/J-1570-2015/
SC https://scopus.com/authid/detail.uri?authorId=57192961558

Sergiy Plankovskyy
sergiy.plankovskyy@kname.edu.ua

D.Sc., Professor
Department of Automation and Computer-Integrated Technologies
O. M. Beketov National University of Urban Economy in Kharkiv, Kharkiv, Ukraine
iD https://orcid.org/0000-0003-2908-903X
P https://publons.com/researcher/H-6120-2015/
SC https://www.scopus.com/authid/detail.uri?authorId=24473286300

Volodymyr Kombarov
volodymyr.kombarov@kname.edu.ua

Ph.D., Associate Professor
Department of Automation and Computer-Integrated Technologies
O. M. Beketov National University of Urban Economy in Kharkiv, Kharkiv, Ukraine
iD https://orcid.org/0000-0002-6158-0374
SC https://www.scopus.com/authid/detail.uri?authorId=57211793853

Lidiia Piddubna
lidiya.piddubna@kname.edu.ua

Ph.D., Associate Professor
Department of Automation and Computer-Integrated Technologies
O. M. Beketov National University of Urban Economy in Kharkiv, Kharkiv, Ukraine
iD https://orcid.org/0000-0002-4225-1612
P https://publons.com/researcher/L-7161-2016/
SC https://www.scopus.com/authid/detail.uri?authorId=57331472000